Seismic Performance of Steel Pipe Sheet Pile Foundation on Soft Ground

Tongxiang, An, Osamu Kiyomiya & Thanh Trung
Waseda University, Japan

SUMMARY:
The vibration behaviour and seismic performance of a typical bridge pier steel pipe sheet pile foundation were investigated by nonlinear dynamic response analysis in this study. The foundation was built on a soft surface ground that was a clay layer with a SPT value of 3 and a depth of 21 m. The analysis was carried out by taking into account the effects of soil-structure interaction and non-linear properties of the soil and the joints between the pipes. In order to investigate the influence of the 2011 Off the Pacific Coast of Tohoku Earthquake on the seismic performance, the ground motion recorded during this Earthquake was considered as well. As a result, the soil-structure interaction and the joint nonlinear properties affect the vibration behaviour and the seismic performance of the bridge pier and the steel pipe sheet pile structure. The influence on the seismic performance of the input wave used in this study from the 2011 Off the Pacific Coast of Tohoku Earthquake is limited.

Keywords: seismic performance; steel pipe sheet pile foundation; soft ground; soil-structure interaction; 2011 Off the Pacific Coast of Tohoku Earthquake

1. INTRODUCTION

Because of the difference in stiffness between soil and foundation structure, and the inertia of the foundation structure, almost all the foundation structures including caisson, pile and steel pipe sheet pile etc., and soil interact under seismic excitation. Up to now, the study on soil-structural interaction (SSI) has been carried out mostly focused on pile foundation, and some results show that SSI can elongate the natural period and increase the damping of the structures. It is conservative if the effect of SSI is neglected in the seismic design. However, the recent research results and the observations of earthquake damage show that the SSI caused an increase in the seismic response of structures especially for the response displacements of structures. Steel pipe sheet pile (SPSP) is composed of a steel pipe and couplings welded on the side/sides of the steel pipe. The interlocking of the coupling of the steel pipe sheet pile links SPSP to construct SPSP foundation and the interlocked couplings form the joints of SPSP structure. With strong stiffness, large bearing capacity and trustworthy construction, SPSP structures have been widely used as the foundations of large scale bridges, especially in cases that the bridge spans a river or a bay where the surface ground is very weak and/or the water is very deep. As a flexible structure, the seismic performance of SPSP foundation is affected by the seismic interaction of soil and structure especially in cases that the structure was built on soft ground. Given the interaction of soil and structure, and the non-linear behaviour of soil, steel pipe and the pipe joint may yield during earthquakes, meaning the dynamic response of SPSP structures are extremely complex and not yet clearly understood. In current Japanese "Seismic design specifications for highway bridges", the steel pipe sheet pile foundation and soil are modelled as a couple of linear concentrated springs for the structure analysis, and the reaction forces of the springs are used as the loads to design the foundation structures, i.e. the seismic effect of soil-structure interaction and the nonlinear properties of the soil, joint and steel pipe are not completely taken into account in the structural seismic analysis and design. It is significant to appropriately verify the effects of the interaction between soil and steel pipe sheet pile structure, and the nonlinear properties of the soil and

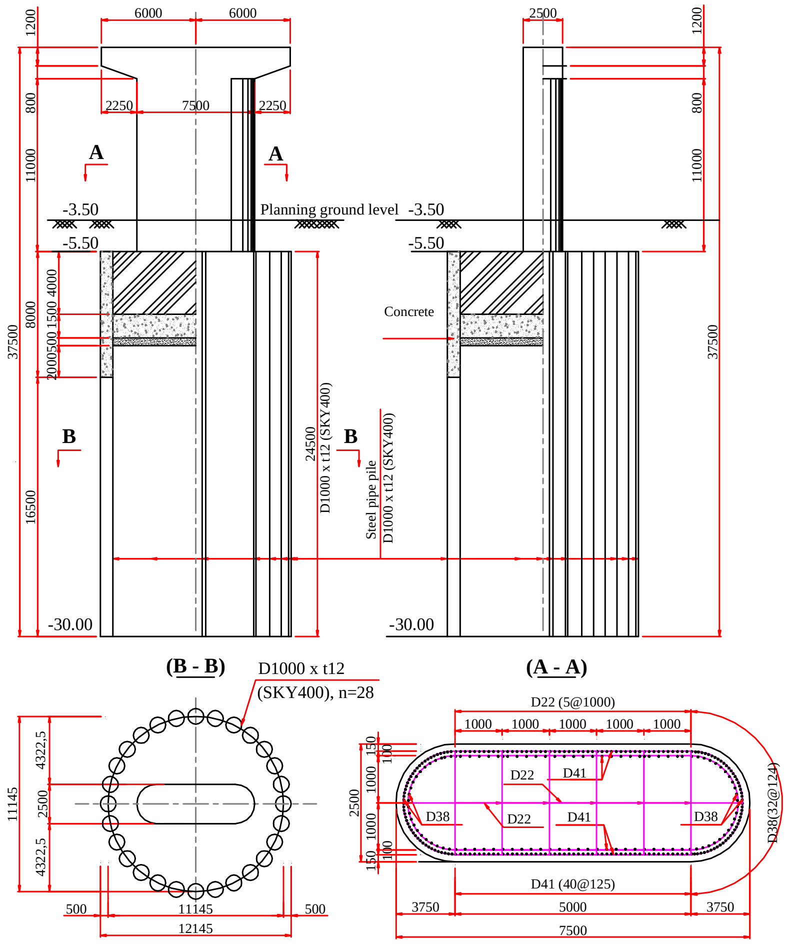

Figure 2.1. Prototype bridge pier-SPSP foundation

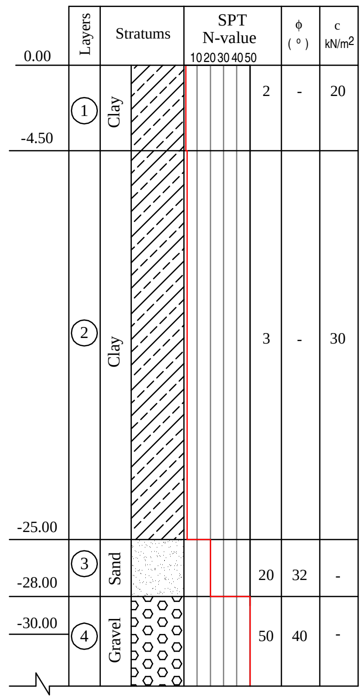

Figure 2.2. Soil condition

joint on structural seismic analysis and design. In this study, the vibration behaviour and seismic performance were verified on a typical SPSP bridge pier foundation built on soft ground by considering the effect of SSI and the nonlinear properties of the SPSP, and the influence of the SPSP joint properties on the seismic performance was investigated as well. Besides that the seismic wave recorded during the 2011 Off the Pacific Coast of Tohoku Earthquake (hereinafter referred to as the 2011 Tohoku Earthquake) was also considered in this work.

2. PROTOTYPE BRIDGE PIER-SPSP FOUNDATION-SOIL SYSTEMS

A typical steel pipe sheet pile supported highway bridge pier as shown in **Figure 2.1** was considered for this work that was demonstrated in “Materials for Seismic Design of Highway Bridges”. It was one of the pier foundations of a 5-span continuous steel plate girder bridge. The foundation consisted of 28 steel pipes forming the outside wall of a diameter of 11.145 m jointed by joint pipes. The steel pipes with a diameter of 1000 mm were driven to a depth of 20.5 m below the pile cap that had a thickness of 4.0 m and a diameter of 12.145 m. The joint pipe had a diameter of 165.2 mm. The material of the pipes was SKY400. The pier was constructed of reinforced concrete with a typical T shape. The height of the pier was 13.0 m including the overhanging part. The column was 11.0 m high with an oval section of 2.5×7.5 m. The strengths of the concrete and reinforcement were 21 MPa and 295 MPa (yielding), respectively. The main reinforcement was arranged in two rows with the space of around 125 mm for the outside and 250 mm for the inside. The diameters of the reinforcement were 41 mm for the straight part and 38 mm for the circular part. The tie hoop reinforcement with a diameter of 22 mm was spaced at 150 mm in vertical direction. The concrete was effectively confined with a length of 100 mm both in longitudinal and transverse directions. The superstructure weights supported by the consideration pier were 7,850 kN, 7,100 kN and 4,740 kN in longitu- dinal, vertical and transverse direction, respectively. The surface ground comprised 4 layers as shown in **Figure 2.2**. The first layer

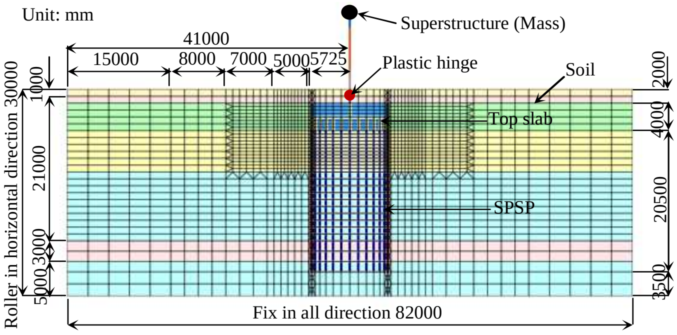

Figure 3.1. SPSP-Soil model

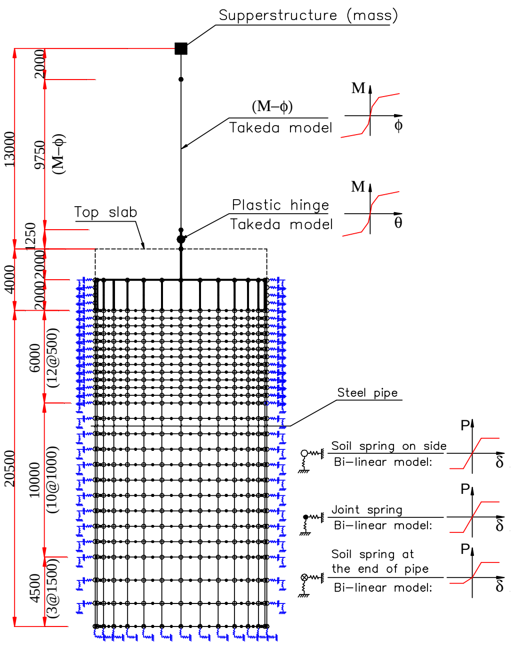

Figure 3.2. SPSP-Spring model

was a soft clay layer with an average SPT value of 2, which adhesion was 20 kN/m^2. Its density was 1,600 kg/m^3 and depth was 1.0 m. The second layer was also a clay layer with an average SPT value of 3 and adhesion of 30 kN/m^2. It had a depth of 21.0 m and the density of 1,700 kg/m^3. A sand layer with an average SPT of 20 and angle of inner friction of 32 degrees was followed. It had a depth of 3.0 m and its density was 1,800 kg/m^3. The base ground was a gravel layer where the average SPT value was 50 and inner friction angle was 40 degrees. Its density was 2,000 kg/m^3.

3. MODELLING METHODOLOGY

This work focused on investigating the effect of soil-SPSP interaction and the joint mechanics properties on the vibration behaviour and seismic performance of the bridge pier with SPSP foundation, the earthquake was assumed to be applied in one direction, moreover, the soil was treated as nonlinear element, for convenience, the prototype bridge pier was modelled as a 2D model. Here, the foundation was represented by two types of analysis model. One was that the soil around the SPSP structure was directly introduced into the model and the SPSP was supported by soil element as shown in **Figure 3.1** (hereinafter referred to as SPSP-Soil Model), i.e. not only the rigidity and the strength of the soil but the mass and the dissipation damping of the soil were taken into account in this model. The other was that the surrounding soil was represented by bilinear springs and the SPSP was supported by soil springs as shown in **Figure 3.2** (hereinafter referred to as SPSP-Spring Model), i.e. the stiffness and the strength of the soil were considered but the mass and the dissipation damping were neglected in this model. This was one of the recommended models for seismic design used for large scale earthquake by the current Japanese highway bridge seismic design specifications. As to the SPSP-Soil Model, the soil was represented by plane strain elements. The constitution relationship between shear stress and shear strain of soil was assumed to be nonlinear and defined by a modified Ramberg-Osgood model. The soil elements at the bottom of the model were assumed to be fixed in all directions and that at the two sides were assumed to be roller in horizontal direction in the dynamic analysis. As to the SPSP-Spring Model, the soil springs were elasto-plastic with consideration of the sliding, pushing and gapping between the pipes and soil. The coefficient of subgrade reaction used to calculate the stiffness of the soil was determined by Equations 3.1 and 3.2 for horizontal direction of front face and vertical direction of the bottom of the SPSP foundation.

$$k_H = \alpha_k k_{HO} (B_e / 0.3)^{-3/4} = \alpha_k (E_D / 0.3)(B_e / 0.3)^{-3/4} \tag{3.1}$$

$$k_V = k_{VO} (B_V / 0.3)^{-3/4} = (E_D / 0.3)(B_V / 0.3)^{-3/4} \tag{3.2}$$

Where, k_H : coefficient of horizontal subgrade reaction for SPSP front face; k_{HO} : reference value of the coefficient of subgrade reaction in horizontal direction calculated by Equation 3.3; α_k : correction

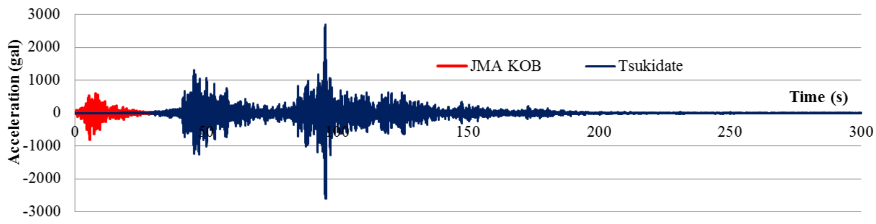

Figure 4.1. Input ground motions

factor of coefficient of subgrade reaction (taken to be 1.5 here); B_e : equivalent loaded width; k_V : coefficient of vertical subgrade reaction; k_{VO} : reference value of the coefficient of vertical subgrade reaction calculated by Equation 3.4; B_V: equivalent loaded width of foundation; E_D : dynamic modulus of deformation of the ground obtained by Equation 3.3

$$E_D = 2(1+\nu_D)G_D = 2(1+\nu_D)\gamma_t V^2{}_{SD} / g \tag{3.3}$$

Where, ν_D : dynamic Poisson's ratio of the ground; G_D : dynamic shear deformation modulus of the ground; γ_t : unit weight of the ground; V_{SD} : shear elastic wave velocity of the ground; g :acceleration of gravity. The yield strength of the springs depends on the inner friction angle for sand soil and the cohesive strength for clayey soils. The upper limit of horizontal ground reaction in front of the foundation was calculated by Equation 3.4.

$$p_{Hu} = \alpha_p p_{Ep} \tag{3.4}$$

Where, p_{Hu} : upper limit of horizontal unit ground reaction force at foundation front; α_p : overdesign factor of horizontal unit ground reaction force; p_{Ep} : passive soil pressure intensity during earthquake. The steel pipes were modelled with beam elements that interact with the surrounding soil through a series of normal and shear coupling springs. The joint pipes were modelled with normal and shear coupling springs. The nonlinear property of these coupling springs was elasto-plastic. The pile cap was modelled using plane strain elements with concrete properties and beam elements for the SPSP-Soil Model and SPSP-Spring Model, respectively. These elements interact with the surrounding soil elements through interface elements made of a series of normal and shear springs that connect the opposing surfaces at the interacting nodes. The bridge pier was modelled using beam elements. A plastic hinge was introduced into the bottom of the pier column to evaluate the bending performance of the column. The bending nonlinearity including the flexural cracking, yielding and the hysteretic behaviour of the plastic hinge and the column of the pier was considered by the Takeda model.

4. INPUT GROUND MOTIONS

Acceleration time history was used as the input ground motion. Two earthquake records as shown in **Figure 4.1** were considered in this work. They were recorded on open stiff ground. One of them was specified in "Seismic design specifications for highway bridges" for Level 2 seismic design, it was from 1995 Hyogokennabu Earthquake (intraplate type earthquake), named JMA KOB wave. The maximum acceleration was 812 gal and the lasting time was 30 s. Another record was from 2011 Off the Pacific Coast of Tohoku Earthquake at Tsukidate in Miyagi, named Tsukidate wave. The wave was comprised of two main motions. The peak acceleration of the first main motion was 1320 gal and that of the second main motion was 2,700 gal, and the total lasting time was 300 s. The input ground motion was applied at the bottom of the soil layer in the dynamic analysis for SPSP-Soil Model and for SPSP-Spring Model was exerted at the soil springs using multi-point input method.

5. ANALYTICAL METHOD AND VERIFICATION PROCEDURE

Nonlinear dynamic analysis method was applied in this work. The analysis was performed by direct time history integral calculus method. The integration was conducted by Newmark-β (β = 0.25) method and the time interval of integration was 0.001 s. In addition, the Rayleigh's damping was adopted in the dynamic analysis. The coefficient of Rayleigh type damping was calculated by strain energy damping ratios.

To conduct the analysis on the SPSP-Spring Model, the ground motion inputs were firstly calculated under seismic excitation on the soil model which was the model excluded the structural part from SPSP-Soil Model. The horizontal displacements at the position of soil springs were used as the ground motion input for the SPSP-Spring Model. The eigen-value analyses were then carried out on the SPSP-Soil Model and the SPSP-Soil Model. Time history nonlinear dynamic analyses were subsequently conducted on the two models. Finally, the oscillation behaviour and seismic performance of the bridge pier and SPSP foundation were verified according to the dynamic analysis results. The influence of the SPSP joint properties and the 2011 Off the Pacific Coast of Tohoku Earthquake on the seismic performance was investigated by the dynamic analysis results on SPSP-Soil model.

Table 5.1 shows the analytical cases of this work. "Normal" indicated that the recommended stiffness and upper limit resistance of the joint were adopted. In this case the shearing stiffness and the upper limit resistance were 1,200,000 kN/m^2, and 200 kN/m, respectively. Joint stiffness and joint resistance indicated that the stiffness and the upper limit resistance were used as parameters to conduct the dynamic analysis. The stiffness and the upper limit resistance of the joint were assumed to be 10 times larger than that of the normal case in this work. When the joints were damaged, i.e. the case that the stiffness of the joints was "0" was analysed as well. The normal case of the SPSP-Soil Model calculated by the JMA KOB wave was referred to as SPSP-Soil, and that calculated by the Tsukidate wave was referred to as Tsukidate. The normal case of the SPSP-Spring Model was referred to as SPSP-Spring. The 10 times stiffness case and the 10 times upper limit resistance case were referred to as J-Ten-Stiffness and J-Ten-Resistance, respectively. The "0" stiffness case was referred to as J-0-Stiffness.

Table 5.1. Analytical Cases

	SPSP-Soil Model			SPSP-Spring Model
	Normal	Joint Stiffness	Joint Resistance	Normal
JMA KOB	○	○	○	○
Tsukidate	○			

6. EIGEN-VALUE AND VIBRATIONAL MODE

Eigen-value was calculated by subspace method, and until the 50th vibration mode was calculated. As an example, the results of the longitudinal direction were taken up to present. The principal vibrational modes in longitudinal direction (X direction) calculated on the SPSP-Soil case and SPSP-Spring case were shown in **Figure 6.1**. The first mode of the SPSP-Soil was both of the fundamental modes of the structure and the soil, i.e. the structure was its flexural vibration and the soil was its shear vibration. As for the SPSP-Spring case, the first mode was its flexural vibration. As shown in Table 6.1, the effective mass ratio of the first mode for the SPSP-Soil case was 64.8% and that for SPSP-Spring case was 68.9%. The first mode was dominant for both of the two cases. The natural frequency of the SPSP -Soil case was 1.248 Hz and that of the SPSP-Spring case was 1.985 Hz. The ratio between them was 1.00:1.59. The 8th vibrational mode for SPSP-Soil case was a combination of the second mode of the structure and the soil. Its frequency and effective mass ratio was respectively 3.575 Hz and 6.5%. As to the 2nd mode of the SPSP-Spring case, the natural frequency was 5.683 Hz and the effective mass ratio was 27.5%. From this point of view, the mass of the soil shortens the natural frequency and changes the effective mass, significantly affects the dominant vibrational mode of the structure.

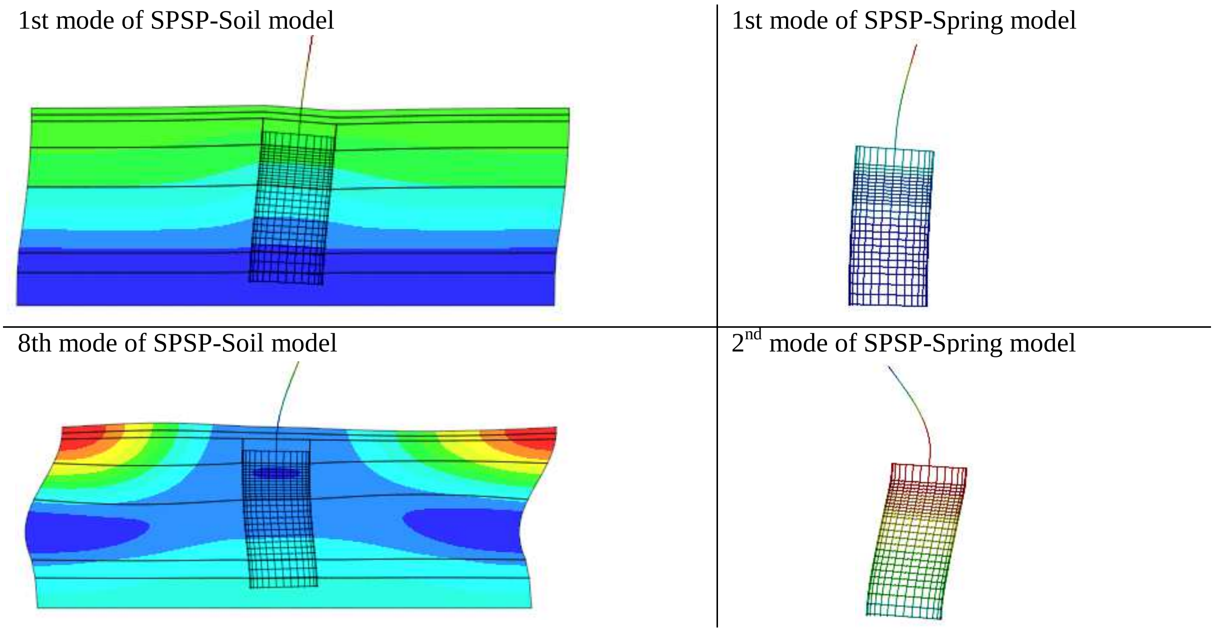

Figure 6.1. Principal vibrational modes

Table 6.1. Eigen-Value of Principal Modes in Longitudinal Direction

SPSP-Soil Case				SPSP-Spring Case			
Mode	f (Hz)	P. F. -X	E. Mass Ratio	Mode	f (Hz)	P. F. -X	E. Mass Ratio
1	1.2481	188.750	64.80%	1	1.9845	45.4960	68.92%
3	2.2698	33.214	2.01%	2	5.6834	28.7490	27.52%
4	2.6431	28.127	1.44%	4	21.2151	6.7021	1.50%
8	3.5752	59.571	6.45%	7	51.1955	5.7944	1.12%

7. RESPONSES OF SUPERSTRUCTURE

Focusing on the response displacement and acceleration of the superstructure, the vibration behaviour of the bridge pier was investigated. The time history responses of the displacement were shown in **Figure 7.1**. The maximum displacement of the SPSP-Soil case was 0.334 m and that of the SPSP-Spring case was 0.472 m. The ratio between them was about 1.00:1.42, i.e. the SPSP-Spring case calculated lager displacement than the SPSP-Soil did. It is thought that the mass and the dissipation damping of the soil decreased the response displacement of the superstructure. The maximum displacement calculated by the Ten-Stiffness case and J-0-Stiffness case was respectively 0.411 m and 0.338 m, comparing that calculated by the SPSP-Soil case, there is a tendency that the enlargement of the stiffness of the pipe joint increases the response displacement of the superstructure, while the reduction of stiffness has little effect on the response displacement. When the upper limit resistant force of the pipe joint was increased by 10 times (the J-Ten-Resistance case), the response displacement of the superstructure reached 0.629 m, it is 1.89 times bigger than that of SPSP-Soil case, i.e. the increase of the upper limit resistant force of the pipe joint enlarges the response displacement of the superstructure. It is because that the increase of the upper limit of the resistance makes the joint within elastic state and the energy cannot dissipate via the joint yielding. The maximum response displacement calculated by the Tsukidate wave was 0.167 m. It was half of that caused by the JMA KOB wave. The influence on the displacement of the superstructure by Tsukidate wave was limited. As shown in **Figure 7.1**, the maximum response accelerations calculated by the SPSP-Soil and SPSP-Spring were 7.32 m/s^2 and 10.06 m/s^2, respectively, i.e. the mass and the dissipation damping of the soil decreased the response acceleration of the superstructure by 37%. The J-Ten-Stiffness, J-Ten-Resistance and J-0-Stiffness calculated the maximum response accelerations of 7.21 m/s^2, 7.93 m/s^2

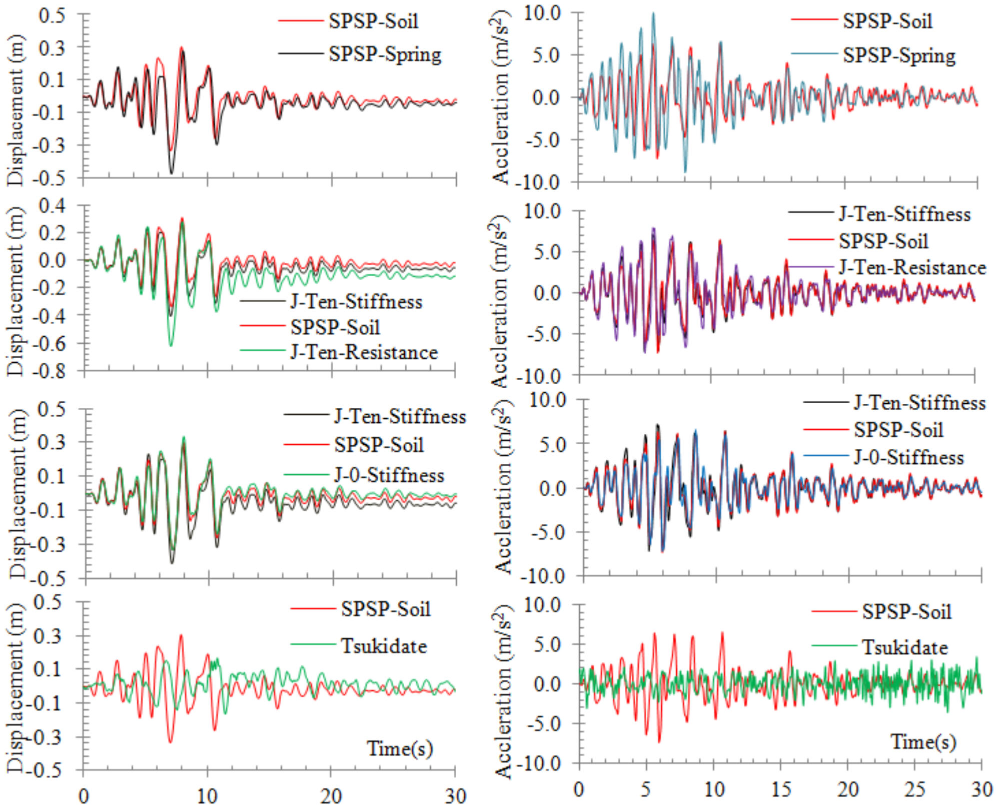

Figure 7.1. Time history responses of the superstructure

and 7.21 m/s^2, respectively. Comparing with the SPSP-Spring case, there were little differences in maximum response acceleration of the superstructure among these cases, i.e. the joint mechanics properties had little effect on the response acceleration. The maximum acceleration caused by the Tsukidate wave was 3.56 m/s^2, which was less than that calculated in the SPSP-Soil case. The influence on the acceleration of the super-structure by Tsukidate wave was limited.

8. SEISMIC PERFORMACE

The seismic performance of the structure was verified based on the dynamic responses of the pier column and SPSP structure. The longitudinal direction results were introduced.

8.1. Seismic performance of pier column

Focusing on the dynamic responses of the plastic hinge, the shear forces of the column and the residual displacement at the position of the superstructure, the seismic performance of the column was verified. The hysteresis loops of the bending moment against the rotational angle of the plastic hinge were shown in **Figure 8.1**. The main rebars at the plastic hinge were calculated yielding by all the other cases except the Tsukidate case. The maximum rotational angle of the SPSP-Soil case was 6.29 mrad and that of the SPSP-Spring case was 10.04 mrad, their ratio was 1.00:1.60, i.e. a bigger rotational angle was calculated by SPSP-Soil case, the mass and the dissipation damping of the soil reduced the rotational angle of the plastic hinge by 60%. In case that the stiffness of the pipe joint was enlarged by 10 times (J-Ten-Stiffness case), the maximum rotational angle (9.18 mrad) increased by 1.46 times. When the joint was damaged and the stiffness was 0 (J-0-Stiffness case), the maximum rotational angle was 7.10 mrad which increased by 1.13 times. The stiffness of the pipe joint affected the seismic behaviour of the plastic hinge. The maximum rotational angle of the J-Ten-Resistance was 17.63 mrad. It was 2.80 times bigger than that of SPSP-Soil case. The upper limit resistant force of the pipe joint affected the seismic behaviour of the plastic hinge as well. The rebars at the plastic hinge

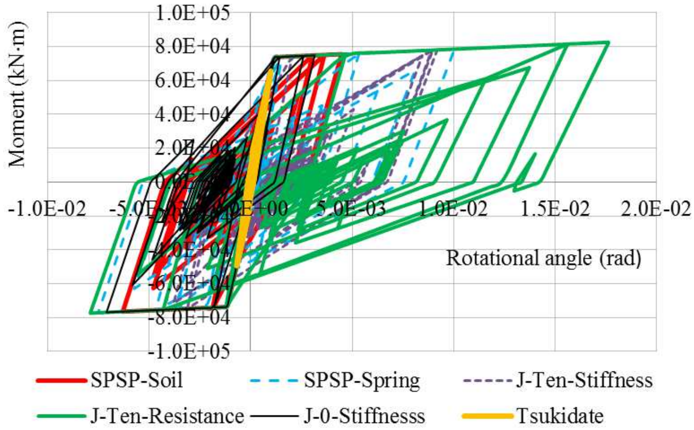

Figure 8.1. Hysteresis loop of bending moment against rotational angle of plastic hinge

was still within the elastic state under the Tsukidate wave. The influence on the seismic behaviour of the plastic hinge by Tsukidate wave was limited. In addition, the upper limit rotational angle of the plastic hinge was 22.85 mrad, i.e. all the responses were less than the limit.

The maximum shear force S_{mas}-C of the pier column (shown in Table 8.1) of the SPSP-Soil and the SPSP-Spring were 7947 kN and 11495 kN, respectively. The mass and the dissipation damping of the soil reduced the shear force of the pier column by 1.45 times. The J-Ten- Stiffness, the J-Ten-Resistance, the J-0-Stiffness and the Tuskidate case calculated the maximum shear force of the pier column of 8496 kN, 9120 kN, 8195 kN and 5956 kN, respectively. The soil mass and dissipation damping largely reduced the shear force, while the damage of the pipe joint, the enlargement of the joint stiffness and the upper limit resistance increased the shear force of the pier column. The upper limit shear force was 19965 kN, i.e. all the responses were less than the limit.

The residual displacement D_r-C of the pier column of the SPSP-Soil, the SPSP-Spring, the J-Ten-Stiffness, the J-Ten-Resistance, the J-0-Stiffness and the Tuskidate case was respectively 0.051 m, 0.118 m, 0.084 m, 0.215 m, 0.055 m and 0.004 m as shown in Table 8.1. The soil mass and dissipation damping largely reduced the residual displacement, while the damage of the pipe joint slightly, the enlargement of the joint stiffness and the upper limit resistance largely increase the residual displacement of the pier column. The upper limit residual displacement was 0.130 m, i.e. the residual displacement of J-Ten-Resistance case went beyond the limit.

Table 8.1. Shear Force and Residual Displacement of the Pier Column, Displacement of Top Slab

	SPSP-Soil	SPSP-Spring	J-Ten-Stiffness	J-Ten-Resistance	J-0-Stiffness	Tsukidate
S_{max}-C(kN)	7947	11495	8496	9120	8195	5956
D_r-C (m)	0.051	0.118	0.084	0.215	0.055	0.004

8.2. Seismic performance of SPSP

The sectional forces of the pile and the reaction forces at the bottom of the pile were used to verify the performance of the SPSP structure. The sectional force distribution of the leftmost pile was shown in **Figure 8.2**. As to the compressive axial forces, the maximum value was calculated at the intermediate part of the pile because of the resistance of the pipe joints, except the J-0-Stiffness case. The maximum compressive axial force of SPSP-Soil case and SPSP-Spring case was respectively 3810 kN and 5270 kN. The ratio between them was 1.00:1.38. The mass and the dissipation damping of the soil reduced the maximum compressive axial force of pile. The J-Ten-Stiffness case calculated a maximum compressive axial force of 4180 kN, while the J-0-Stiffness case calculated that of 3376 kN. With the enlargement of the stiffness of the pipe joint, the compressive axial force of the pile increased. The maximum compressive axial force of the J-Ten-Resistance case was 5026 kN. It was 1.32 times bigger

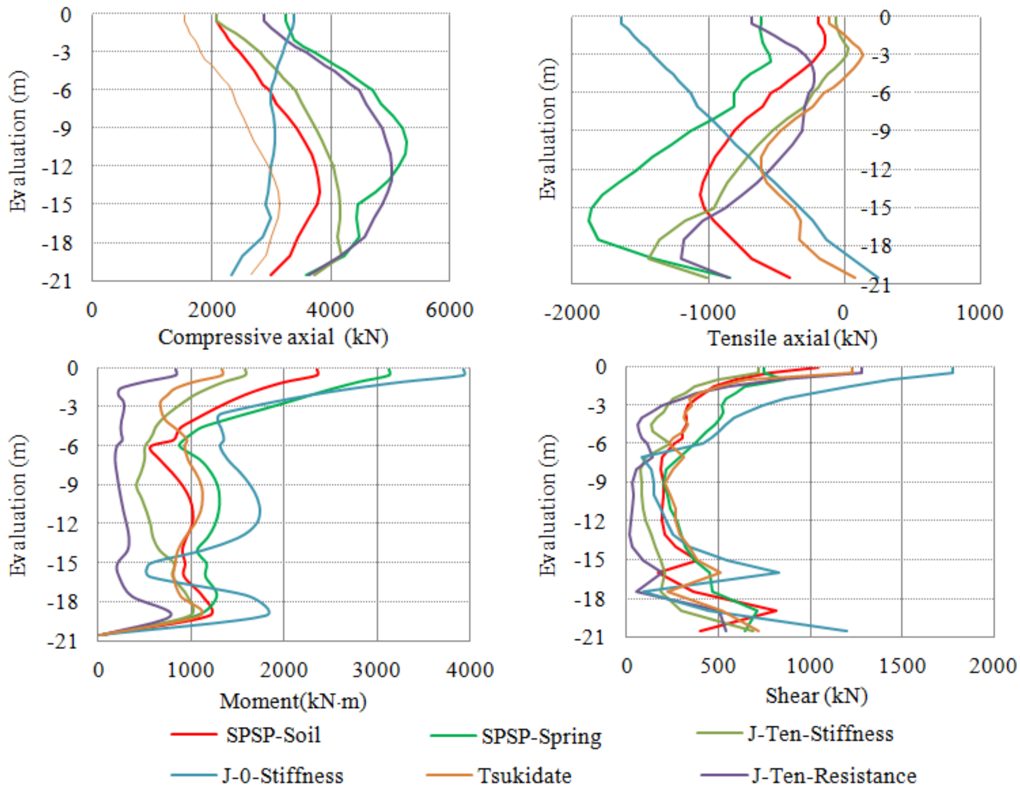

Figure 8.2. Sectional forces distribution of the pile

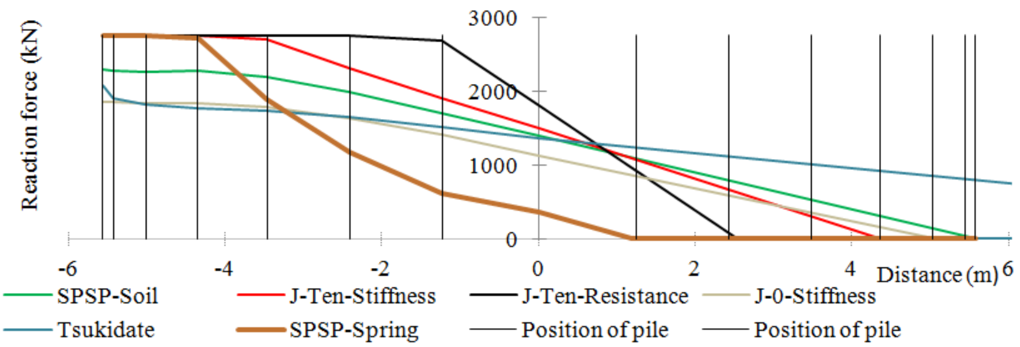

Figure 8.3. Vertical reaction forces at the ends of the pile

than that of the SPSP-Soil case. The enlargement of the upper limit of the resistant force of the pipe joint increased the compressive axial force of the pile. The Tsukidate wave caused a maximum compressive axial force of the pile of 3145 kN. As to the tensile axial force, the maximum value of the SPSP-Soil case and the SPSP-Spring case was respectively 1056 kN and 1880 kN. The ratio between them was 1.00:1.78. The J-Ten-Stiffness case calculated a maximum tensile axial force of 1443 kN, while the J-0-Stiffness case calculated that of 1642 kN. The maximum tensile axial force of the J-Ten-Resistance case was 1196 kN, which was 1.13 times bigger than that of the SPSP-Soil case. The enlargement of the upper limit of the resistant force of the pipe joint increased the tensile axial force of the pile. The Tsukidate wave caused a maximum tensile axial force of the pile of 611 kN. As to the fluctuation range of the axial force of the pile, the calculation of the SPSP-Soil, the SPSP-Spring, the J-Ten-Stiffness, the J-Ten-Resistance, the J-0-Stiffness and the Tuskidate case was 4866 kN, 7150 kN, 5623 kN, 6222 kN, 5018 kN and 3756 kN, respectively. The soil mass and the dissipation damping reduce the fluctuation range of the pile axial force. The joint damage, the enlargement of the joint stiffness and upper limit resistance increase the fluctuation range of the pile axial force. The influence on the fluctuation range of the pile axial force by Tsukidate wave is limited. The maximum shearing force of the SPSP-Soil, the SPSP-Spring, the J-Ten-Stiffness, the J-Ten-Resistance, the J-0-Stiffness and the Tuskidate case was 1043 kN, 855 kN, 718 kN, 1277 kN, 1775 kN and 1228 kN, respectively. The damage of the pipe joint increases the shearing force of the pipe. The maximum bending moment of the SPSP-Soil, the SPSP-Spring, the J-Ten-Stiffness, the J-Ten-Resistance, the J-0-Stiffness and the Tuskidate case was 2353 kNm, 3130 kNm, 1574 kNm, 835 kNm, 3925 kNm and 1331 kNm, respectively. The soil mass and dissipation damping, and the enlargement of the joint stiffness and the upper limit resistance largely reduce the pipe bending moment, while the damage of the pipe joint largely increases the pipe bending moment.

The maximum and minimum vertical reaction forces at the end of the piles were shown in **Figure. 8.3**. The outermost pile was uplifted (minimum reaction force was 0 kN) at the end, but the ground did not yield (maximum reaction force was less than 2758 kN) for SPSP-Soil case. However, for the SPSP-Spring case, piles from the outermost side to the structural centre were uplifted and the ground where from the other outermost side pile to the fourth column pile went beyond its bearing capacity. The enlargement of the pipe joint stiffness and upper limit resistance increased the uplift piles and made the ground yield. The damage of the joint increased the uplift piles. The influence on the pile reaction force by Tsukidate wave was limited.

9. CONCLUSION

The main findings in this work were as follows: 1) The model including the soil significantly shortens the dominant natural frequency of the structure. The mass and dissipation damping reduce the responses of the superstructure, the pier column and the SPSP structure, and serve a function in favour of the seismic performance of the structure; 2) The enlargement of the pipe joint stiffness increases the pile reaction forces, the responses of the superstructure and the pier column, but reduces the pile bending moment; 3) The enlargement of the upper limit resistance of the pipe joint largely reduces the pile bending moment, but affects the response of the superstructure and the seismic performance of the pier column; 4) The damage of the pipe joints has little effect on the response of the superstructure, while largely affects the seismic performance of the substructure especially the SPSP structure; 5) The influence on the vibrational behaviour and seismic performance of the 2011 Earthquake wave used in this study is limited.

REFERENCES

Wolf, J.P. (1985). Dynamic Soil-Structure interaction, Prentice-Hall, Inc., Englewood Cliffs, New Jersey.

Mylonakis G., and Gazetas G. (2000). Seismic soil–structure interaction: beneficial or detrimental? , *Journal of Earthquake Engineering*, **Vol. 4, Issue 3**, 277–301.

Mylonakis G., Gazetas G., Nikolaou S. and Michaelides O. (2000). The role of soil on the collapse of 18 piers of the Hanshin Expressway in the Kobe Earthquake, *12th World Conference on Earthquake Engineering*, New Zealand, 1074.

Tuladhar R., Mutsuyoshi H. and Maki T. (2008). Seismic Behavior of concrete bridge pier considering soil-pile-structure interaction, *The 14th World Conference on Earthquake Engineering*, **No. 02-0075**, October, Beijing, China, 12-17

Boris J., Sashi K., and Feng X. (2004). Influence of soil-foundation-structure interaction on seismic response of the I-880 Viaduct, *International Journal for Engineering Structures*, **Vol. 26, Issue 3**, 391-402

Khalil L., Sadek M., and Shahrour I. (2007). Influence of the soil–structure interaction on the fundamental period of buildings, *Earthquake Engineering and Structural Dynamics*, **Vol. 36**, 2445–2453.

JRA-2002, (2002). Specification for highway bridge, part IV: Substructures & part V: Seismic design, Japan Road Association.

Kyoshin network (K-net) system, *National Research Institute for Earth Science and Disaster Prevention (NIED)*, Japan.

Veletsos AS. and Meek JW. (1974). Dynamic behavior of building-foundation systems. *Earthquake Engineering and Structural Dynamics,* **Vol. 3, No. 2**, 121–138.

An T.X., Kiyomiya O. Hung T. V. and Kochi R. (2011). Nonlinear dynamic analysis of soil-steel pipe pile sheet-structure interaction under seismic excitation, *Proceedings of the 35th International Symposium on Bridge and Structural Engineering*, jointly organized by IABSE-IASS, London, UK